Mon. Not. R. astr. Soc. (1989) **240**, 957–974

Numerical experiments on radial virial oscillations in *N*-body systems

M. David and T. Theuns★ *University of Antwerp (RUCA), Theoretical Mechanics and Astrophysics, Groenenborgerlaan 171, 2020 Antwerpen, Belgium*

Accepted 1989 April 6. Received 1989 April 5; in original form 1989 February 16

Summary. Initially uniform and spherical bound systems of mass points exhibit radial pulsations on a dynamical time-scale, analogous to adiabatic pulsations in stars. Starting from the Identity of Lagrange, Chandrasekhar & Elbert derived relations for the period and amplitude of these oscillations. We present results of numerical experiments on these pulsations in *N*-body systems. In quiet systems starting near virial equilibrium, the amplitude of the pulsations is small and they are long lived. In this case, the life time depends strongly on the number of particles. Collisional effects and mixing eventually lead to damping. Violent oscillations turn out to be self-destructive. It is shown how these pulsations can produce escapers.

1 Introduction

Global pulsations of a gravitationally bound *N*-body system are collective motions characterized by the fact that global quantities measuring the linear dimension of the system, oscillate around their virial values. Such pulsations have been studied previously by several authors. Lynden-Bell (1967) predicted them after linearization of the Identity of Lagrange, so that his solution was valid only for small amplitude oscillations. Chandrasekhar & Elbert (1972) solved the complete non-linear equation for a spherical mass distribution, under the assumption of homologous evolution. We show that these oscillations are in fact the analagy of the ones found by Ledoux (1945), in an adiabatic ideal gas, in the context of radial stellar pulsations.

From the observational point of view, these oscillations are important for the determination of cluster masses (Aarseth & Saslaw 1972), in the context of the dynamical evolution of young open clusters (Verschueren & David 1989) and for the study of systems which have suffered strong collapse. Theoretically they are important for better understanding the process of violent relaxation.

Numerically, the pulsations were encountered in several studies on the dynamical mixing of orbits in collisionless systems, e.g. Bouvier & Janin (1970), Cuperman, Harten & Lecar (1971), Severne & Luwel (1985). The latter two papers concern one-dimensional systems but the

★Research assistant of NFWO (National Foundation for Scientific Research, Belgium).

argument leading to an equation for the pulsations and to an expression for their period is easily adapted to this case.

In the present paper, we investigate these global radial pulsations by means of numerical experiments on 500-, 1000- and 2000-body systems, each with a $m^{-2.5}$ mass spectrum, which are initially uniform and spherical, with an isotropic velocity distribution and a given virial ratio. Two essentially different codes were used: in the first code (PS), the gravitational force on a particle is calculated using the Poisson solver routines as described by Brandt (1977) and by Monaghan & Varnas (1988); the second code (NB) is one of Aarseth's (1985) standard N-body codes, which is based on direct summation of two-body forces. They are essentially different from the physical point of view in that the two-body forces produced by the Poisson solver tend to zero as two particles approach each other while this is not the case for the other code. The PS code therefore describes a quasi-collisionless model, at least on the time-scales we are interested in.

In Section 2, we rederive the equations describing the oscillations for an N-body system and for an adiabatic gas cloud. In Sections 3 and 4 we present our numerical results and compare them with theory. Section 5 contains some remarks on non-uniform initial states. The conclusions are summarized in Section 6.

2 Virial oscillations

2.1 NOTATIONS

We consider a system of N mass points, with masses m_n, positions $\mathbf{r}_n$ and velocities $\mathbf{v}_n$ with respect to the centre of mass frame. Following Chandrasekhar (1942), we define a characteristic linear dimension R of the system, using its potential energy $U(<0)$

$$R=-\frac{GM^2}{2U}, \tag{1}$$

where M is the total mass and G the gravitational constant. For a homogeneous and spherical mass distribution, $R=\frac{5}{6}$ of the radius of the system.

Similarly, the total kinetic energy K defines the mass-weighted rms velocity V

$$V=\sqrt{\frac{2K}{M}}. \tag{2}$$

The total energy E of a bound system defines the virial values K_0 and U_0, of K and U, i.e.

$$K_0=|E|,\ U_0=2E \tag{3a}$$

to which correspond virial values for V and R

$$V_0=\left(\frac{2|E|}{M}\right)^{1/2},\ R_0=\frac{GM^2}{4|E|}. \tag{3b}$$

These in turn can be used to define the 'crossing time' or 'dynamical time'

$$t_{\rm cr}=\frac{2R_0}{V_0}=\left[\frac{G^2M^5}{(2|E|)^3}\right]^{1/2}. \tag{4}$$

A useful parameter to characterize the global state of a bound system is the virial ratio q

$$q=\frac{K}{|U|}=1-\frac{R}{2R_0}. \tag{5}$$

Another linear measure of the size of the system is S, defined by the moment of inertia I

$$S=\sqrt{\frac{I}{M}}, \tag{6}$$

where

$$I=\Sigma m_n r_n^2.$$

Let us define the structure parameter λ as the ratio

$$\lambda=\frac{S}{R}, \tag{7}$$

which equals 0.93 for a homogeneous spherical system. It ranges from 0.93 to 1 for a homogeneous spherical shell, as the inner radius varies from zero to the outer radius. For a two-body system $\lambda=2[m_1m_2/(m_1+m_2)^2]^{3/2}$ which is $\frac{1}{4}$ if the masses are equal, and less otherwise. Note that for an inhomogeneous system the value of R may be dominated by a local mass concentration or even by just one close binary, while the value of S may be dominated by a relatively small amount of mass located far away from the centre. In such cases R and S need not have any relation to each other and they lose their significance as a measure for the linear dimension of the system as a whole; the ratio λ is then next to meaningless. As a final point, note that λ is invariant under a homologous transformation $\mathbf{r}_n \Rightarrow \alpha \mathbf{r}_n$.

2.2 PULSATIONS IN N-BODY SYSTEMS

Using equations (1), (6) and (7) the well known Identity of Lagrange can be written as

$$\frac{M}{2}\frac{d^2S^2}{dt^2}=2E+\frac{GM^2}{2R}=2E+\frac{GM^2\lambda}{2S}. \tag{8}$$

We have already noted that the value of λ does not differ much from one system to another, provided the systems are not too inhomogeneous. If we suppose λ remains constant and equal to λ_0 during the evolution of a given system, (8) becomes an equation for S. This assumption is slightly weaker than Chandrasekhar's assumption of homologous evolution. Equation (8) is identical to the equation for the interparticle distance in a two-body system, if one identifies $SM/\sqrt{m_1m_2}$ with the interparticle distance. Therefore, we can immediately write down the solution for $S(t)$, using the well known parametric form

$$t=\frac{T}{2\pi}[\psi+\psi_0+A\ \sin(\psi-\varphi)] \tag{9a}$$

$$S=S_0[1+A\ \cos(\psi-\varphi)], \tag{9b}$$

where

$$S_0=\frac{\lambda_0 GM^2}{4|E|} \tag{10a}$$

$$\frac{T^2}{S_0^3}=\frac{8\pi^2}{\lambda_0 GM} \quad \text{or} \quad T=\pi\lambda_0 t_{\rm cr}. \tag{10b}$$

Eliminating ψ from (9) and substituting $(3/\pi)^{1/2}$ for λ_0 one immediately recovers the results of Chandrasekhar & Elbert (1972) for a spherical system with an exponential density distribution. The equations (9a and b) describe a global pulsation of the system: the characteristic length S, and therefore also R, oscillates periodically around a value S_0 (resp. S_0/λ_0) with amplitude AS_0 (resp. AS_0/λ_0). Incidentally equation (10b) shows that the relation between the period and the average linear dimension in a global pulsation, may be regarded as an extension of Kepler's Third Law to an N-body system.

The constants ψ_0, A and φ are determined by the state of the system at an initial time t_0 where we choose $\psi=0$

$$\psi_0=\frac{2\pi}{T}t_0+A\sin\varphi \tag{11a}$$

$$A=\sqrt{a^2+b^2}, \qquad \varphi=\arctan\left(\frac{b}{a}\right), \qquad b\sin\varphi\geq 0 \tag{11b}$$

$$a=\frac{S(t_0)}{S_0}-1, \qquad b=\frac{T}{2\pi}\frac{S(t_0)}{S_0^2}\frac{dS}{dt}(t_0). \tag{11c}$$

In a two-body system the parameter A is the excentricity of the orbit and it is directly related to the angular momentum in the centre of mass frame. A similar direct relation between A and the total angular momentum L cannot be established for an N-body system, but there is an inequality derived by Saari (1984) and (independently) by Sergheysels (1986) from which it follows that the magnitude of A is actually limited by the angular momentum. Noting $\mathbf{I}$ for the inertia tensor this inequality is

$$E-U\geq\tfrac{1}{2}\mathbf{L}\cdot(\mathbf{I}^{-1}\mathbf{L}). \tag{12}$$

It states that the total kinetic energy of the system at any time is never less than the kinetic energy of a rigid rotator which has the same angular momentum and the same inertia tensor as the N-body system at that time. Let us assume for a moment that the elements of $\mathbf{I}^{-1}$ behave roughly like $(MS^2)^{-1}$; then it is meaningful to introduce some structure factor μ defined by:

$$\mathbf{L}\cdot(\mathbf{I}^{-1}\mathbf{L})=\frac{\mu L^2}{MS^2}, \tag{13}$$

where, e.g. μ would equal $\frac{3}{2}$ if the system were spherically symmetric. Then one finds in fact that

$$A\leq\sqrt{1-\frac{\mu L^2}{2M|E|S_0^2}}. \tag{14a}$$

Furthermore one may define a characteristic rotation period T_r by

$$L = MS_0^2\left(\frac{2\pi}{T_r}\right) \tag{14b}$$

so that, taking account of equation (10b), the inequality becomes

$$A \leq \sqrt{1-\mu\left(\frac{T}{T_r}\right)^2}, \tag{14c}$$

which provides a clear qualitative picture of the constraint imposed on the pulsation by the angular momentum: if the angular momentum is increased the period T_r decreases so the amplitude of possible pulsations decreases as well. Of course, expression (14c) will be significant as a constraint, only if the individual angular momenta of the mass points in the system all have more or less the same direction; otherwise the constraint imposed by the individual angular momenta is likely to be much more important than expression (14c).

2.3 RADIAL OSCILLATIONS IN AN ADIABATIC, SELF-GRAVITATING GAS-SPHERE

We briefly recall the equations governing the dynamics of radial adiabatic motion in a self-gravitating gas: (see, e.g. Cox & Giuli 1968)

$$\begin{aligned}
&\frac{\partial\rho}{\partial t}+\rho\frac{1}{r^2}\frac{\partial}{\partial r}r^2v_r=0\\
&\frac{\partial v_r}{\partial t}=-\frac{1}{\rho}\frac{\partial P}{\partial r}-\frac{Gm}{r^2}\\
&\frac{\partial\varepsilon}{\partial t}=\frac{P}{\rho^2}\frac{\partial\rho}{\partial t}\\
&P=K\rho^{\gamma}.
\end{aligned} \tag{15}$$

The time derivatives are convective; $\rho=\rho(r,t)$ denotes the density at radius r at time t, while P and ε denote the (scalar) pressure and thermal energy per unit mass, respectively. They are connected by the equation of state

$$P=(\gamma-1)\rho\varepsilon. \tag{16}$$

v_r is the radial component of the fluid velocity and m is the mass interior to radius r:

$$m=\int_0^r 4\pi a^2\rho(a,t)\,da. \tag{17}$$

In the case of small deviations from hydrostatic equilibrium, the linearized equations permit homologous oscillations if the equilibrium model is homogeneous (Cox & Giuli, equation 27.67). The period Π of these oscillations is given by

$$\begin{aligned}
&\Pi=\frac{2\pi}{C}\\
&C^2=(3\gamma-4)\frac{4\pi}{3}G\rho_0,
\end{aligned} \tag{18a}$$

where ρ_0 is the (constant) density of the homogeneous model. For an ideal gas, $\gamma = \frac{5}{3}$, we find

$$\Pi = \sqrt{\frac{3\pi}{G\rho_0}}. \tag{18b}$$

This gas cloud is also in virial equilibrium in the sense of equation (3a), if we identify the total thermal energy of the cloud, with the kinetic energy K. If we take the analogy still further and calculate the 'crossing time' for this cloud, equation (4), we find (R_* denotes the radius of the cloud)

$$t_{\rm cr} = \left(\frac{5}{3}\right)^{3/2} \sqrt{\frac{R_*^3}{GM}} = \left(\frac{5}{3}\right)^{3/2} \sqrt{\frac{3}{4\pi\rho G}},$$

so, from equation (18b) we obtain

$$\Pi = 2\left(\frac{3}{5}\right)^{3/2} \pi t_{\rm cr}, \tag{19}$$

which is the same as for the uniform stellar gas. We conclude that the oscillations found in the stellar gas are the equivalent of the well-known radial adiabatic homologous pulsations that exist in self-gravitating ideal gas-spheres.

3 Numerical experiments

3.1 THE SIMULATION PROGRAMS

Two different N-body codes were used to investigate the oscillations numerically. The first one will be designated by PS and is a (real space) Poisson-solver code. This code was originally developed to calculate the self-gravity in SPH calculations (Monaghan & Varnas 1988). The density and force assignment schemes are designed to conserve linear and angular momentum and a predicted Euler method is used to do the time stepping. This code represents a quasi-collisionless model over the time-scales we are interested in. The other code (NB) is Aarseth's standard NBODY2 code (Aarseth 1985). The forces in NB are softened with the 'standard' value for the softening parameter (4R/N).

3.2 THE INITIAL CONDITIONS

The initial state of the systems we studied is characterized essentially by the initial virial ratio $q(0)$. The initial mass and velocity distribution was always the same, up to a scale factor depending on $q(0)$: the N mass points were given random positions within a sphere of radius 1 and random velocities within a spherical shell between 10 and 11 in velocity space. The initial velocity vectors were restricted to such a thin shell in order to avoid the occurrence of excessive sub-clustering in the early stages of the evolution. Afterwards, all dynamical quantities were scaled in the customary way for N-body calculations, i.e. total mass, gravitational constant and total energy equal to N, 1 and $-\frac{1}{4}N^2$, respectively, and $q = q(0)$. In virial equilibrium, $q(0) = \frac{1}{2}$, which implies $R_0 = 1$, $V_0 = (N/2)^{1/2}$. Transformation back to physical units is effected by multiplying all lengths with the actual virial radius for the system at hand

(e.g. in parsecs), and by multiplying the time with γ, given by

$$\gamma \approx \left(\frac{NR_0^3\,(\mathrm{pc})}{M(M_\odot)}\right)^{1/2} \times 10^7 \text{ yr}. \tag{20}$$

Finally, in the illustration and discussion we shall express time in units of the crossing time and velocity in units V_0 which have a direct physical relevance, along with R_0 which naturally appears as the unit of length under the scaling conditions mentioned above. Positions and velocities are always referred to the centre of mass system.

3.3 QUIET AND VIOLENT SYSTEMS

Numerical experiments during the last two decades (see, e.g. Aarseth 1973, 1985 and references therein) have revealed many important characteristics of the dynamical evolution of gravitational N-body systems. In particular, it is well known that a bound system with uniformly distributed initial positions and velocities within a sphere, develops a core–halo structure after a space of time which depends mainly on the number of mass points. The energy-spread increases and if there is a broad mass spectrum the heavier bodies tend to move closer to the centre while the lighter ones are more likely to be found on wide excentric orbits (i.e. in the halo). The formation of hard and heavy binaries in the core and the escape of stars from the system through few body interactions, may be regarded as extreme cases of this behaviour.

If N is sufficiently large and if the system is 'quiet', i.e. if it is set into motion with $q=0.5$ and with an isotropic velocity distribution which is cut off well below the escape velocity, then the structure change occurs fairly gradually: its onset – as judged from the increase of the structure parameter λ– becomes apparent on a time-scale of the order of the collisional relaxation time T_E defined by Chandrasekhar (1942, equation 5.217★). Substituting in his expression (from equations 3b and 4) $t_{cr}=(8R_0^3/GM)^{1/2}$ we get

$$T_E = \frac{\sqrt{3\pi}}{64}\,\frac{N}{\ln(N/2^{3/2})}\,t_{cr}. \tag{21}$$

Some typical values (in units t_{cr}) are given in Table 1. One should recall here that the derivation of equation (21) is valid only for systems with a sufficiently large number of particles so that the values quoted for $N=50$, 100 are, at best, merely indicative. A more realistic estimate for the relaxation time in small systems was discussed by McMillan, Casertano & Hut (1988).

Table 1. Relaxation time in units of the dynamical time.

N	50	100	200	500	1000	2000
T_E	0.8	1.3	2.3	4.6	8.2	14.6

On the other hand, if the initial virial ratio is much different from 0.5 the system will undergo violent relaxation (Lynden-Bell 1967); the binding energy and the velocity of individual mass points may change drastically under the influence of the strong variations both in space and time of the mean field in this case. In particular a core–halo structure (though

★This equation was derived using the virial radius R_0 as the average radius of the system. One might argue that in the case of a uniform sphere the real radius of the sphere should be used instead; in that case the expression of T_E would be multiplied by $(6/5)^3$ and in the logarithm, $2^{3/2}$ would be replaced by $(5/3)^{3/2}$.

different from the one produced by collisional evolution, e.g. by the fact that violent relaxation does not lead to mass segregation) and possibly a number of escapers are produced on a time-scale of the order of T, given by equation (10b). An extensive review of the mechanisms of violent relaxation is given by Saslaw (1985).

In systems with N of the order of 100 or less, besides the effects of numerous weak interactions (collisional relaxation) and of mean-field fluctuations, close two- and three-body interactions often cause a drastic structure change. They may, in fact, at any odd time, produce some hard binary and/or some energetic escaper and, as pointed out before, even a few of these may be sufficient to rob the quantities R and S of their significance as characteristic lengths for the system as a whole. Moreover, hard binaries absorb binding energy (Heggie 1975) and may eventually drive small systems towards complete disruption. From a series of numerical experiments we found that the effects of close encounters are too strong in systems with $N \leq 200$ for global pulsations as described by equation (9) to occur, while this was not the case in systems with $N \geq 500$ (at least until the formation of a dense core).

Since the prediction of global pulsations is based on the assumption that λ remains constant or exhibits at most small random fluctuations, the formation of a core–halo structure is likely to inhibit the pulsations, at least in the form of equation (9). Therefore, whenever a global pulsation occurs one expects it to be much weakened after the relaxation time T_E (in a quiet system) or after one period T (in violent systems). In particular it follows that pulsations with a sufficiently large amplitude to constitute 'violent motion', must be self-destructive. Global pulsations which persist for more than one period can thus be expected to occur only with relatively small amplitudes and in systems with a relaxation time of at least a few periods T.

The breakdown of strong pulsations which appears within the framework of equation (8) as a consequence of core–halo formation, can be understood dynamically as the result of Landau damping (i.e. the transfer of energy from a collective mode to individual bodies) and of phase mixing among the objects taking part in the collective motion.

3.4 RESULTS

Fig. 1 shows the occurrence of pulsations in system A, which started from virial equilibrium. (For a summary of calculated systems, see Table 2.) The origin of the pulsation in this case is explained in Section 4.2. The functions S and R are seen to oscillate in phase with the same amplitude $\cong 7$ per cent, and consequently, their ratio λ remains almost constant. The $R(t)$ curve exhibits an initial lump around 1.5 crossing times. The origin of this effect is purely kinematical and will be treated in more detail below; it is present in all calculations using the 'uniform initial state', but it is most conspicuous in system A. In Fig. 1(b) we have superposed the synthetic $S(t)$ curve, which was calculated using equation (9). This figure shows clearly that the period is in good agreement with equation (9), although the real 'period' is slightly longer

Table 2. Summary of experiments.

	N	q	t	Code
A	2000	.5	10	PS
B	2000	.4	26	PS
C	500	.4	10	NB
D	1000	.4	10	NB
E	2000	.4	10	NB
F*	2000	.2	20	NB
G*	2000	.2	20	PS

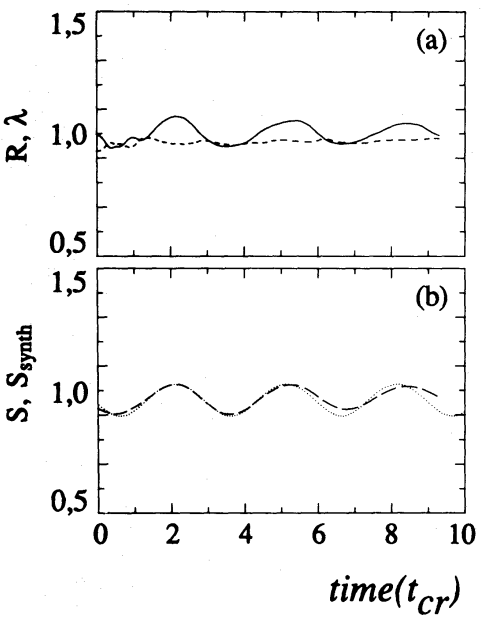

Figure 1. System A ($N=2000$, $q(0)=0.5$): (a) characteristic radius R (solid line) and ratio S/R (dashed line); (b) characteristic radius S (long dashed) and synthetic S (dotted).

and not exactly constant. We used the state of the system at 2 crossing times to determine the value of the parameters A, α and λ; the parameters A, and λ, as calculated from (11) at a given instant t_0, turn out to be sufficiently insensitive to t_0 to allow the prediction of the amplitude at any other instant.

The moderate collapse situation of system B is shown in Figs 2. Mark the longevity of these pulsations, persisting for more than 20 crossing times. The amplitude in the initial state is $\cong 20$ per cent but decreases quickly during the early stages. After six crossing times, it remains fairly constant, $\cong 6$ per cent, and decreases very slowly towards the end of the run.

The period of these pulsations is not constant, but exhibits fluctuations of the order of 10 per cent around its mean value of 3 crossing times ($\langle\lambda\rangle=0.96$). One can see that R and S are not always in phase. At the end of the run, one notices a slight expansion of the system as a whole.

The collective nature of the pulsation is seen in Fig. 2(b) in the behaviour of the Lagrangian radii containing 20, 40 ... 80 per cent of the total mass. These radii oscillate homologously and in phase over the observed period of time. Fig. 2(c) shows that the radial velocity, averaged over a shell bounded by two subsequent Lagrangian radii, exhibits the same behaviour in each of the shells. This collective feature is the more remarkable because the radial velocity dispersion inside a given shell is much larger than the typical radial velocity of this shell, as can be seen in Fig. 2(d).

In Fig. 3, we compare systems with 500, 1000 and 2000 particles (systems C, D and E, respectively), which started with the same virial ratio. They were integrated with a direct summation code (NB). It can be seen that the oscillations tend to live longer in systems with more particles. System C ($N=500$) undergoes a moderate initial collapse and subsequent expansion. Afterwards, R and S fluctuate but S is dominated by an almost linearly increasing contribution due to escaping particles and/or particles moving into the halo. The curves of system D ($N=1000$) appear more smooth and the onset of a second pulsation can be seen. The linear trend in S can still be discerned but is much less pronounced. In system E ($N=2000$), the oscillations are more persistent still. If we compare this figure with Fig. 2(a), we

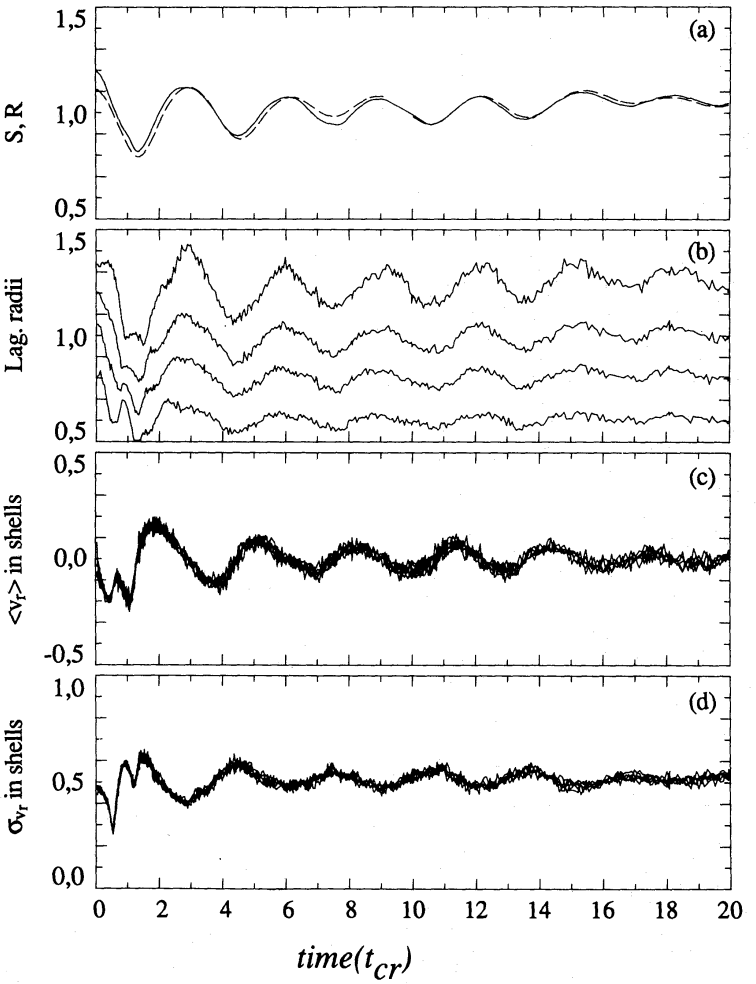

Figure 2. System B ($N=2000$, $\dot{q}(0)=0.4$): (a) linear dimensions R (solid line) and S (long dashed); (b) time evolution of Lagrangian radii containing 20, 40, 60 and 80 per cent of the total mass; (c) radial velocity averaged over Lagrangian shells (superposition of five curves, each pertaining to 20 per cent of the total mass) and (d) same as in (c) for the radial velocity dispersion.

can remark that the pulsation is more heavily damped in the case of the direct summation code, and the linear trend in S is more pronounced.

The violently collapsing systems F and G (Fig. 4), which start from the same initial state, exhibit perfectly the same global behaviour for at least 4 crossing times; up to about 3 crossing times their S versus t curves also agree very well with the synthetic S curve (superposed in Fig. 4a), except for the maximal collapse factor, which apparently is overestimated by equation (10). In the PS calculation (Fig. 4b) the escapers were removed as soon as they reached a distance of $7R_0$ from the centre of mass, in order to prevent the interpolation grid from expanding indefinitely; this removal accounts for the somewhat irregular behaviour of $R(t)$ between 4 and 10 crossing times and for the fact that $S(t)$ does not exhibit the familiar monotonously increasing trend.

For $t>10$ crossing times, the number of particles turned out to remain constant; here $R(t)$ again oscillates smoothly, contrary to its behaviour in the corresponding era of the NB results. As can be seen from the Lagrangian radii in Fig. 4d, this quiet oscillation is a remnant of the original violent one, which persists in the PS calculation but is damped out completely in the NB calculation (see Fig. 4c). The quiet oscillation in Fig. 4(b) has a markedly smaller period than for example the one in Fig. 1; this will be discussed further on.

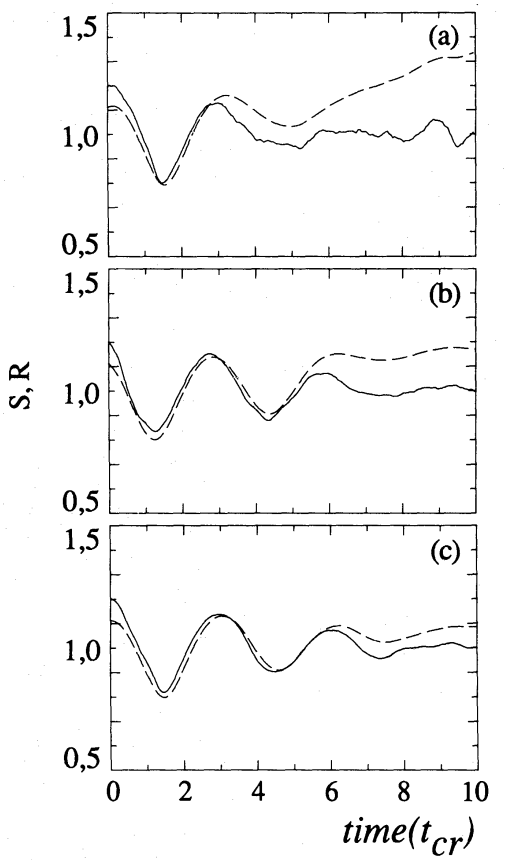

Figure 3. Time evolution of the characteristic radii S (dashed) and R (solid) in systems starting with virial ratio 0.4: (a) 500 particles (system C); (b) 1000 particles (system D) and (c) 2000 particles (system E).

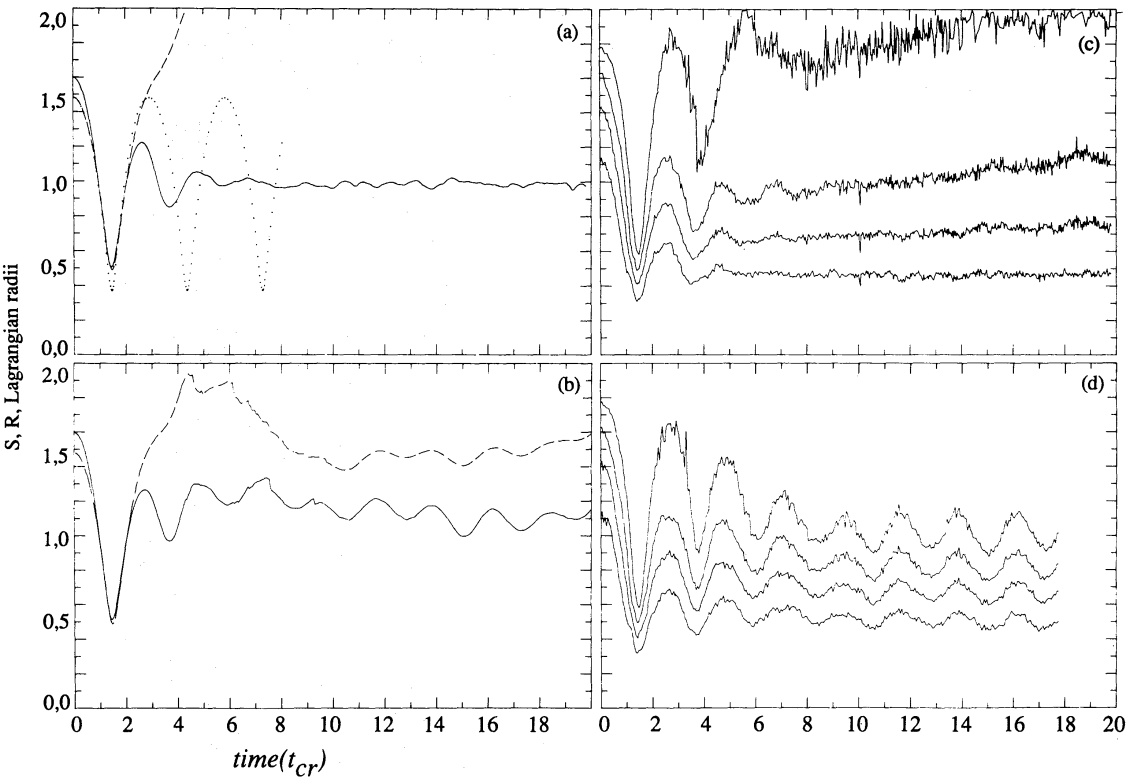

Figure 4. Collapse situation with $N=2000$, $q(0)=0.2$, characteristic radius R (solid line), S (dashed line) and synthetic S (dotted line): (a) for system F; (b) for system G; (c) Lagrangian radii for system F and (d) Lagrangian radii for system G.

4 Discussion

4.1 THE LIFE OF GLOBAL PULSATIONS

It is well known that an N-body system becomes increasingly 'collisionless' on the scale of a crossing time, as N increases (*cf.* equation 21). As argued in Section 3.3, the life of a small-amplitude global pulsation will therefore increase with increasing N. This is illustrated by Figs 3(a)–(c). Considering these diagrams in reverse order, they illustrate the fact that an increase of the influence of collisions (by decreasing N) leads to quicker damping of the oscillations and to the generation of a more pronounced halo on the same time-scale.

The longevity of the pulsations in Figs 1 and 2(a) is explained by the fact that the Poisson-solver code makes the system almost collisionless. Extrapolating the results in Fig. 3 we may therefore say that Figs 1 and 2 are representative of the behaviour of systems with a very much larger number of mass points.

As expected, the violent pulsation in Fig. 4(a) and (b) is self-destructive, at least as far as the original system as a whole is concerned. However, the Lagrangian radii in Fig. 4(c) show that the inner parts of the system actually continue the oscillation (albeit with a strongly reduced amplitude) up to at least six crossing times which, according to Fig. 3(c) is about the maximal duration of pulsations as allowed by collisions in a system of that size. That is confirmed in Fig. 4(d) where the collisionlessness of the PS-model apparently allows the weak pulsations of the inner parts to go on for a long time. These observations suggest that we are actually dealing with a 'global' pulsation of a *subsystem* of the original system. In order to verify this we analysed the evolution for $t > 10t_{cr}$ in detail. The PS-calculation for system G is possibly unreliable for $t > 4t_{cr}$ due to a considerable expansion of the grid (despite the removal of escapers). Therefore, we analysed the quiet oscillations of Fig. 4(b) using NB with the rest of system G in its state at $10t_{cr}$ as input. This supplementary experiment produced similar quiet oscillations as shown in Fig. 5. The fact that $S(t)$ remains considerably larger than $R(t)$, while exhibiting only very weak fluctuations, and the fact that the period of $R(t)$ is much smaller than $3t'_{cr}$ (t'_{cr} being the proper crossing time of the reduced system), both indicate that the halo

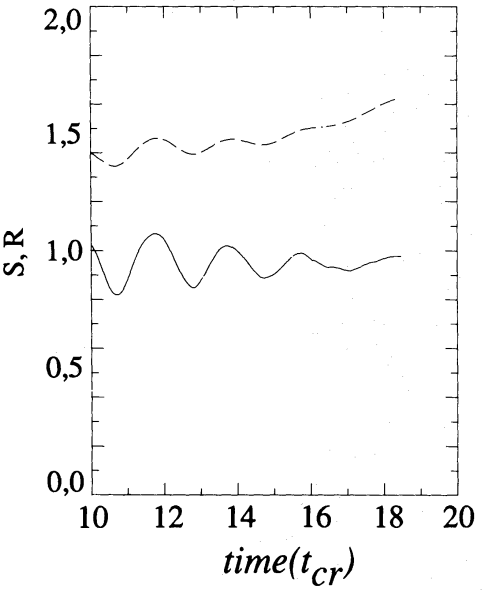

Figure 5. Evolution of the characteristic radii R (solid line) and S (dashed line) for the system consisting of the remaining 1890 particles of system G at $10t_{cr}$; the results were obtained using NB with the PS-results at $10t_{cr}$ as input.

formed after the violent phase does not participate in the radial pulsation. In fact, comparing different open subsystems defined by, respectively, the Lagrangian radii corresponding to 70, 75, 80, 85 and 90 per cent of the original mass, we found that the part of the system confined within the 80 per cent radius, regarded as a subsystem, exhibited both an almost constant λ value (0.98) and an almost constant total energy (-0.805×10^{6}); it contained on average 1575 particles with a standard deviation of 6. The pulsation period of this subsystem, if it were isolated, would be $2.36t_{cr}'$ which is in fair agreement with the period of $2.2t_{cr}'$ one determines visually from Fig. 5.

4.2 THE EFFECT OF THE INITIAL STATE

During the first crossing time one sees, in some figures, fluctuations on a time-scale which is much shorter than a pulsation period. These can be explained as follows. During a time interval which is a small fraction α of the relaxation time one can expect that the orbit of an individual body deviates something of the order α per cent from the orbit it would have if its motion were determined merely by the mean field. Considering the relaxation times involved, as well as the initial conditions of system A, the global behaviour in such systems during, say, the first crossing time, can be approximated by the global behaviour of a set of non-interacting mass points, moving in the gravitational field produced by a uniform sphere of radius $\frac{6}{5}R(t)$. The orbits of such mass points are ellipses centred on the centre of the sphere, as long as they remain inside it; for those that have enough energy to move out of the sphere, the orbit becomes Keplerian as they cross the boundary.

Fig. 6(a) shows the initial state in phase space (r, v_r). Superposed are collisionless orbits of two particles picked from the initial state. The figure illustrates that for the orbits shown, only certain phases of the particles along their orbits can be realized in the initial state, while others cannot. The effect of this on the pericentric arrival times is shown in Fig. 6(b) where two groups of particles can be discerned, the first group arriving around 0.5 crossing times and the second one around 1.5 crossing times. It is the pericentric arrival of these groups which accounts for the early fluctuation in the R- and λ-curves of Fig. 1. Moreover, this selection, together with random fluctuations – which may cause $dS/dt(t_0)$ in equation (11c) to differ from zero – triggers the oscillations in systems starting in (or very near) virial equilibrium (e.g. system A).

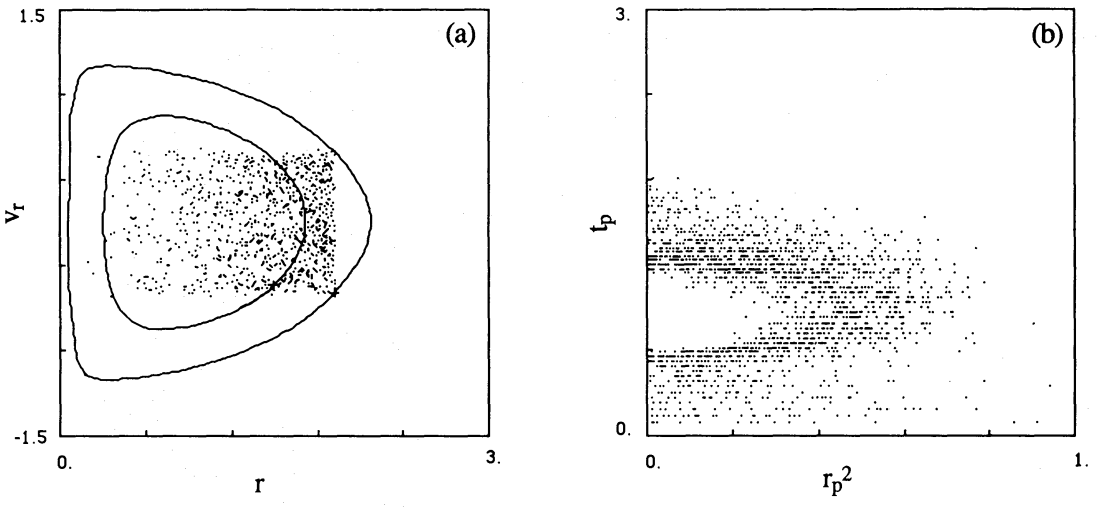

Figure 6. (a) Initial conditions in phase space (r, v_r). Superposed are collisionless orbits for two particles picked from this state. (b) Pericentric arrival time t_p versus pericentric distance (r_p) squared for system $G[q(0)=0.2]$.

A quick numerical check shows that the selection has a similar effect if R is allowed to decrease in time, according to equation (9). So also the lumps in Fig. 2 in the early stages of some of the Lagrangian radii, and the sharp peaks at the beginning of the $v_r(t)$ and $\sigma_r(t)$ curves are a spurious effect caused by the mean field and the particular choice of the initial conditions.

4.3 ENERGY TRANSFER

Mass points may gain so much energy from large amplitude collective modes that they escape from the system (Hénon 1964). This is well understood qualitatively, but the simple analytical model (9) allows us to establish a more quantitative picture of the energy transfer. Let us consider the idealized case of a test mass moving inside a uniform spherical mass distribution with mass M and radius R_S. At a distance $r_* < R_S$ from the centre, the probe is subject to the potential Φ given by

$$\Phi = -\frac{GM}{2R_S}\left[3-\left(\frac{r_*}{R_S}\right)^2\right] \tag{22}$$

and if R_S changes with time the energy per unit mass of the probe will change according to

$$\frac{\partial \varepsilon_*}{\partial t} = \frac{3GM}{2R_S^2}\left[1-\left(\frac{r_*}{R_S}\right)^2\right]\frac{dR_S}{dt}$$

$$= 6\frac{|E|}{M}\frac{R_0}{R_S^2}\left[1-\left(\frac{r_*}{R_S}\right)^2\right]\frac{dR_S}{dt}, \tag{23}$$

where E is the total energy of the mass sphere and R_0 is defined by (3b). One sees immediately that the test mass will gain or lose energy according to whether the sphere is expanding or contracting, the rate of energy transfer being highest in the centre.

Let us assume now that the sphere exhibits a global pulsation. Then, substituting $R_S = \frac{6}{5}R$ and using (7), (9) and (10) we obtain

$$\frac{\partial \varepsilon_*}{\partial t} = \frac{10}{\lambda_0}\frac{|E|}{M}\left[1-\left(\frac{r_*}{R_S}\right)^2\right]\frac{-A\sin(\psi-\varphi)}{[1+A\cos(\psi-\varphi)]^3}\frac{1}{t_{cr}}. \tag{24}$$

As we are interested in situations with a large energy transfer rate, we consider only the case $r_* \ll R_S$ so that the term $(r_*/R_S)^2$ may be neglected. Then one finds that the energy transfer rate becomes maximal for $\psi = \psi_+$ or $\psi = \psi_-$ given by

$$\psi_\pm - \varphi = \arccos\left(\frac{1-\sqrt{1+24A^2}}{4A}\right) = \pi \pm \Delta (\mathrm{mod}\ 2\pi), \tag{25}$$

which, because of (9) corresponds to

$$t_\pm = t_b \pm \Delta t (\mathrm{mod}\ T), \tag{26}$$

where

$$\Delta t = |t(\psi = \psi_\pm) - t(\psi = \varphi + \pi)|$$

and t_b is the instant of maximal contraction, the bounce. Note that $0 \le \Delta \le \pi/2$ so the maxima of the energy transfer occur in a contracted phase. At $t = t_+, t_-$ the energy gain, respectively

Table 3. Relative energy gain or loss.

A	$\frac{\Delta}{\pi}$	$\frac{\Delta t}{T}$	$\lvert\frac{\partial \epsilon_*}{\partial t}\rvert_{max} / \frac{\lvert E\rvert}{M t_{cr}}$
.1	.41	.19	1.1
.2	.33	.14	2.6
.4	.23	.073	8.3
.6	.16	.034	29
.8	.10	.011	194

energy loss, rate of the test mass is maximal. Table 3 shows some typical values, expressed in dynamical units, for different values of the amplitude. One sees that, if the amplitude is about 0.5 or larger, the probe may gain (or lose) an amount of energy of several times the average binding energy of a point mass in the system, provided the probe remains close to the centre for, say, 0.1 crossing times around t_+.

In practice one thus expects that a number of mass points (which are in a favourable orbit as described above) will gain enough energy to become weakly bound or even to escape from the system, in the expansion phase after a strong collapse; this is illustrated in Fig. 7. The lowest level contains particles which are still (but only very weakly) bound; the upper level contains actual escapers. Notice that the population-increase in the energy-levels shown, is in fact limited to a fairly narrow asymmetric time-interval around the instant t_+ given by equation (26). This mechanism for creating a halo and escapers, will be further investigated in a forthcoming paper.

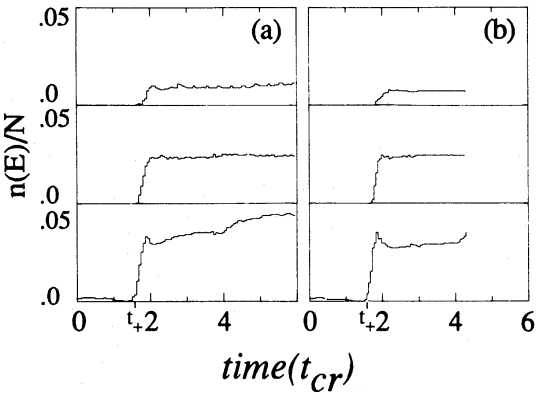

Figure 7. Evolution of the fractional population of energy-classes (from bottom to top) $[-0.3, -0.1]E_p$, $[-0.1, 0.1]E_p$ and $[0.1, 0.3]E_p$, where $E_p = |E|/N$, in (a) system F and (b) system G.

4.4 THE MAXIMAL COLLAPSE

According to several star formation scenarios, a newly formed group of stars or proto-stars is dynamically cool, i.e. the bodies lack, on average, sufficient kinetic energy to sustain the volume in which they were formed. This leads to a global collapse. Extreme collapse situations were studied in detail by Aarseth, Lin & Papaloizou (1988) in systems which were initially uniform, spherically symmetric and at rest. The time of the bounce, t_b, when the collapse factor $C = S_0/S$ becomes maximal, was found to agree with the free fall time t_f, different layers attaining their minimal radius at different instants, with a relatively small spread around t_f.

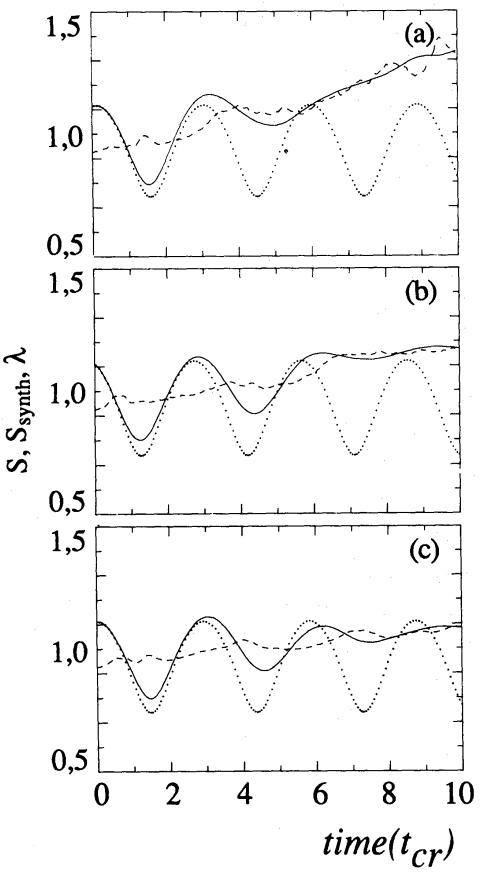

Figure 8. Evolution of the structure parameter λ (dashed line) the characteristic radius S (solid line) and the 'synthetic' S (dotted line) in systems starting with virial ratio 0.4: (a) $N=500$ (system C); (b) $N=1000$ (system D) and (c) $N=2000$ (system E).

In more moderate collapse situations (i.e. with non-zero initial velocities) the time of maximal contraction may be estimated using equations (9), (10) and (11) which should yield a valid approximation provided $T_E \gg t_b$. In particular, if the initial radial velocity distribution is symmetrical with respect to $v_r = 0$, then one has $dS/dt \cong 0$. In order to estimate t_b we then put $\varphi = 0$ in equation (9) and find $t_b = 0.5\,T$, which is easily seen to be equal to the free fall time one would obtain for a uniform spherical system with the same mass and total energy as the system under consideration, but maximally expanded (i.e. $R = 2R_0$, all mass points at rest).

This estimate is seen to agree very well with the numerical value for quasi-collisionless systems (see Fig. 4) while there is a small discrepancy for systems in which collisions influence the dynamics as can be seen in Fig. 8. As a matter of fact, the average slope of the curve of the structure parameter $\lambda(t)$ – which in quiet systems is determined mainly by the effect of collisions – can be related to the shift in t_b by means of a straightforward perturbation calculation, starting from equation (9).

The maximal value of the collapse factor C, as predicted by equation (9) is $C_{max} = 1/(1-A)$; in particular, under initial conditions such that $dS/dt(t_0) = 0$, equations (5) and (11) yield $A = 1 - 2q_0$ so $C_{max} = (2q_0)^{-1}$. The values thus obtained agree well with the experiment in quiet systems but overestimate the maximal collapse factor to an increasing extent as the collapse gets stronger. This is seen both for collisionless and collisional systems. This overestimate was expected, since equations (9) and (11) take account only of the initial velocity dispersion, not of the increase in dispersion due to fluctuations on all scales (Aarseth *et al.* 1988). As the above estimate turns out to be better in situations where the collapse is less strong, it

would seem that these fluctuations (caused by local condensations growing, moving and dissolving) are less powerful in these quiet systems.

5 Non-uniform initial states

A systematic search for virial oscillations in essentially non-uniform systems has yet to be made. We did some preliminary *N*-body calculations for a Plummer-like model, i.e. the initial state was obtained by generating a Plummer-model and rescaling the coordinates and velocities so that $q(0)=0.2$. The results were negative in this case; the deviation from virial equilibrium was damped completely after 3 crossing times (still defined by equation 4) and the evolution was clearly not homologous, the outer parts of the system lagging behind in time with respect to the inner parts. The latter means that Chandrasekhar & Elbert's basic assumption for the prediction of oscillations is strongly violated in this case. Anyway it seems necessary that a further search for virial oscillations in non-uniform systems should be preceded by a search for density and velocity distributions which allow for (approximately) homologous evolution. In a study of instabilities in polytropic systems in virial equilibrium, Barnes, Goodman & Hut (1986) studied a radial instability which caused the Lagrangian radii to oscillate with a period of $1.2t_{cr}$, whereby the inner radii (up to 55 or 60 per cent) moved in antiphase with the outer radii (beyond 70 per cent). From a linear stability analysis the authors concluded that the radial velocity distribution in this case should in fact be bimodal. It is tempting, therefore, to take one step further and to try to explain the observed period in terms of a simple model consisting of two radially pulsating subsystems in antiphase with respect to each other. A quick numerical test using e.g. two equal concentric and uniform spheres, shows that the Lagrangian radii for such a system would indeed behave just like those observed by Barnes *et al.* (in particular, the phase of the radii changes only beyond the 60 per cent radius), the period being half that of the individual spheres. However, in order to establish that both components in such a system may in fact behave according to equation (9), one has to assume that the dynamical coupling between the two is sufficiently weak for some reason. There seems to be no general argument in favour of this.

6 Conclusions

Numerical experiments on initially uniform and spherical bound systems of mass points demonstrate that global radial pulsations, as predicted by Chandrasekhar & Elbert (1972) can survive in these systems, provided the number of mass points is at least of the order of 500. In very quiet systems, such oscillations may be caused by statistical fluctuations in the initial state or by other features (e.g. the selection discussed in Section 4.2) which cause some radial mass motion at the beginning of the evolution. In this case, their amplitude is small (e.g. 6 per cent in Fig. 1) and their lifetime is limited mainly by collisional effects and phase mixing. Therefore they have a longer duration (expressed in crossing times) in larger systems.

In systems starting with a collapse or an expansion, the amplitude is determined primarily by the initial virial ratio. If the initial amplitude is very large, the pulsation is self-destructive and lasts only for about one period; however, small-amplitude oscillations may survive in the inner parts of the system until they are destroyed by collisional effects.

The period of these oscillations (≈ 3 crossing times) is in good agreement with experiment. In a cold collapse situation, the time of maximal collapse is well predicted by the analytic formula but the maximal collapse factor is increasingly overestimated as the collapse gets stronger. The simple analytical expression (9) yields, moreover, a clear insight into the

mechanism by which individual mass points may acquire a large amount of energy from a large-amplitude pulsation and thus move out to form a halo or even escape from the system. In a future paper we intend to concentrate on this aspect of virial pulsations.

Acknowledgments

The authors are indebted to S. J. Aarseth for providing his *N*-body codes, to J. J. Monaghan for providing his SPH-code and to both for many stimulating and useful discussions. Thanks are also due to S. Casertano and D. C. Heggie for their useful comments on a first draft of this paper. This work was partly supported by NFSR (Belgium) grant No. S 2.0091.88. One of us (TT) moreover gratefully acknowledges the hospitality of the Institute of Astronomy (Cambridge, UK) during a month's stay in 1987 and in 1988, and the partial support from the European Astrophysics Doctoral Network enabling these visits.

References

Aarseth, S. J. & Saslaw, B., 1972. *Astrophys. J.*, **177,** 17.
Aarseth, S. J., 1973. *Vistas Astr.*, **15,** 13.
Aarseth, S. J., 1985. In: *Multiple Time Scales,* p. 377, eds Brackhill, J. U. & Cohen, B. I., Academic Press, New York.
Aarseth, S. J., Lin, D. N. C. & Papaloizou, J. C. B., 1988. *Astrophys. J.*, **324,** 288.
Barnes, J., Goodman, J. & Hut, P., 1986. *Astrophys. J.*, **300,** 112.
Brandt, A., 1977. *Math. Comp.*, **13,** 333.
Bouvier, G. & Janin, G., 1970. *Astr. Astrophys.*, **5,** 127.
Chandrasekhar, S., 1942. *Principles of Stellar Dynamics,* Dover Publications.
Chandrasekhar, S. & Elbert, D. D., 1972. *Mon. Not. R. astr. Soc.*, **155,** 435.
Cox, J. P. & Giuli, R. T., 1968. *Principles of Stellar Structure,* Gordon & Breach, London.
Cuperman, S., Harten, A. & Lecar, M., 1971. *Astrophys. Space Sci.*, **13,** 425.
Heggie, D. C., 1975. *Mon. Not. R. astr. Soc.*, **173,** 729.
Hénon, M., 1964. *Ann. Astrophys.*, **27,** 1.
Ledoux, P., 1945. *Astrophys. J.*, **102,** 143.
Lynden-Bell, D., 1967. *Mon. Not. R. astr. Soc.*, **136,** 101.
McMillan, S., Casertano, S. & Hut, P., 1988. *The Few Body Problem, IAU Colloq. No. 96,* p. 313, ed. Valtonen, M. T., Kluwer, Dordrecht.
Monaghan, J. J. M. & Varnas, S. R., 1988. *Mon. Not. R. astr. Soc.*, **231,** 515.
Saari, D. G., 1984. *Cel. Mech.*, **33,** 355.
Saslaw, B., 1985. *Gravitational Physics of Stellar and Galactic Systems,* Cambridge University Press.
Sergheysels, R., 1986. *Cel. Mech.*, **38,** 207.
Severne, G. & Luwel, M., 1985. *Astrophys. Space Sci.*, **122,** 299.
Verschueren, W. & David, M., 1989. *Astr. Astrophys.*, **219,** 105.